Appendix

Appendix A: Dispersion Measurements of Amorphous NH_3/Cu(111)

It was shown previously [Hot99] that the influence of adsorbate layers on the translational symmetry of the Cu(111) surface can be neglected. Therefore, the momentum of photoelectrons parallel to the interfacial plane, $\hbar k_{\parallel}$, is a conserved quantity. The parallel momentum $\hbar k_{\parallel}$ of the photoelectrons depends on the emission angle

$$k_{\parallel}(\varphi, E_{kin}) = \sin\varphi \cdot \sqrt{\frac{2m_e}{\hbar} \cdot E_{kin}} \qquad \text{(A.1)}$$

where m_e is the electron mass, E_{kin} its kinetic energy, and φ the angle between surface normal and detection angle as illustrated by Fig. A.01. In this way, it is possible to determine the dispersion of electronic states by angular-resolved 2PPE measurements. In the present setup, the sample can be rotated by ±16° around the *y* axis. Hereby, the angle of 45° between detector axis and laser beam remains constant.[113]

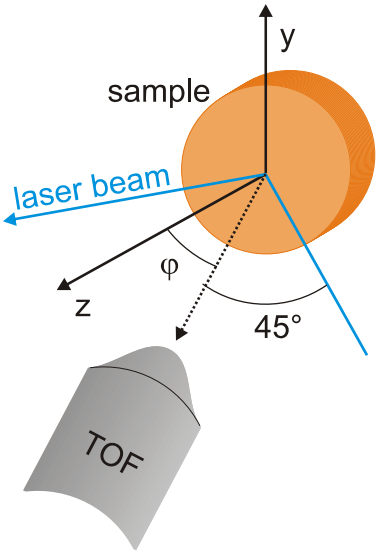

Fig. A.01: *Experimental Setup for Angular-Resolved 2PPE.* The photoemission angle can be varied by rotation of the sample around the *y*-axis. The angle of 45° between detector axis and laser beam remains constant.

The dispersion of an electronic state may be written as the one of a free electron

$$E(\vec{k}) = \frac{\hbar^2 k^2}{2m_{eff}(\vec{k})} \qquad \text{(A.2)}$$

where the effective mass m_{eff} is a measure for the state's localization degree:[114] In the case of delocalized electrons it has a finite value, but becomes infinite for localized states, which exhibit a group velocity of

$$\frac{d\omega}{dk} = \frac{1}{\hbar}\frac{dE}{dk} = 0\,. \qquad \text{(A.2)}$$

[113] The main sources of systematic errors are the opening angle of the spectrometer (7.6°) and wrong alignment of the laser spot on the sample. It has to be exactly on the rotational axis of the surface, as the laser spot otherwise moves on the sample during rotation. A detailed description can be found in [Gah04].

[114] Although it is in principle a tensor, m_{eff} becomes a scalar in front of a surface due to symmerty considerations.

For a state, which is localized parallel to the surface, i.e. with a narrow distribution Δx in real space, a broad bandwidth of $k_{\parallel}$ values is considered according to Heisenberg' Uncertainty Principle. Thus, a flat dispersion anticipated for solvated electrons. However, as shown previously for the electron localization dynamics at the amorphous D_2O/Cu(111) interface, the dispersion of solvated electrons can also *appear* negative. [Bov03, Gah04] This unexpected behavior is explained by the finite bandwidth of the solvated electrons in k-space and the rather broad peaks in energy.[115] As the 2PPE spectra are taken at a specific *angle* and not at a specific $k_{\parallel}$, each spectrum actually corresponds according to equation (A.1) to a parabola in the energy-momentum plane as illustrated by the red curve in Fig. A.02. Thus, a sufficiently broad peak (in energy) can contain a wide $k_{\parallel}$ distribution. Assuming a Gaussian intensity distribution of the solvated electrons along $k_{\parallel}$ with the width $\Delta k_{\parallel}$ and, at first, an energy-*independent* amplitude, as depicted in Fig. A.02, different intensity distributions for different emission angles result: At normal emission ($\varphi = 0$, green curve) the 2PPE spectrum remains unaffected by the finite $\Delta k_{\parallel}$ of the solvated electron. However, at larger angles, the $k_{\parallel}$ distribution leads to a 2PPE intensity decrease towards higher kinetic energies. If now a peak instead of an energy-independent amplitude of e_S is assumed, the finite $\Delta k_{\parallel}$ of the solvated electron leads to a weighting of 2PPE intensity in favor of low kinetic energies. In other words, the maximum of the peak lies at lower energies. This effect can be even stronger, if the $k_{\parallel}$ distribution exhibits an energy dependence. With this approach the authors could show, that the *apparently* negative dispersion corresponded to flat or nearly flat "real" dispersion curves of the solvated electrons. [Bov03, Gah04] The strongest apparently negative dispersion was observed for t = 400 fs: The peak maximum lies at $k_{\parallel}$ = 0.15 Å^{-1} ΔE = 80 meV lower in energy than for $k_{\parallel}$= 0

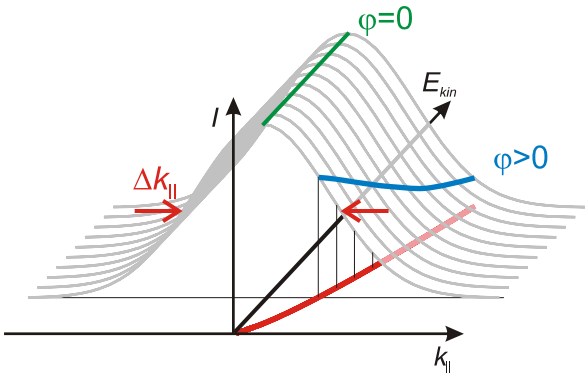

Fig. A.02: *Impact of Finite k-Space Width on 2PPE Intensity.* Adopted from [Gah04]. See text for details.

Angle- and time-resolved 2PPE experiments were also performed for the NH_3/Cu(111) interface. Fig. A.03a depicts, exemplarily, 2PPE spectra at a time delay of 850 fs for a series of emission angles between 0° (normal emission) and 16° (right axis). As apparent from the data, the maximum of the solvated electron distribution shifts with increasing emission angle to *lower* energies. In other words, e_S exhibits an *apparently* negative dispersion. Similar measurements have also been performed for other delay times. The positions of the peak maxima as a function of wave vector $k_{\parallel}$ are depicted in Fig. A.03b. Obviously, the spectral feature of the solvated electrons has a negative dispersion for all time delays investigated, ranging from 10 fs to 5 ps (black curves are a guide to the eye). At all time delays, the effect of the negative dispersion (i.e. the apparent peak shift due to the finite $\Delta k_{\parallel}$) is stronger than for the D_2O/Cu(111) system. The peak maximum lies after 150 fs at $k_{\parallel}$ = 0.15 Å^{-1} ΔE = 110 meV lower in energy than for $k_{\parallel}$= 0.

[115] In the case of D_2O the e_S peak exhibits widths of ~400 meV at kinetic energies less than 1 eV.

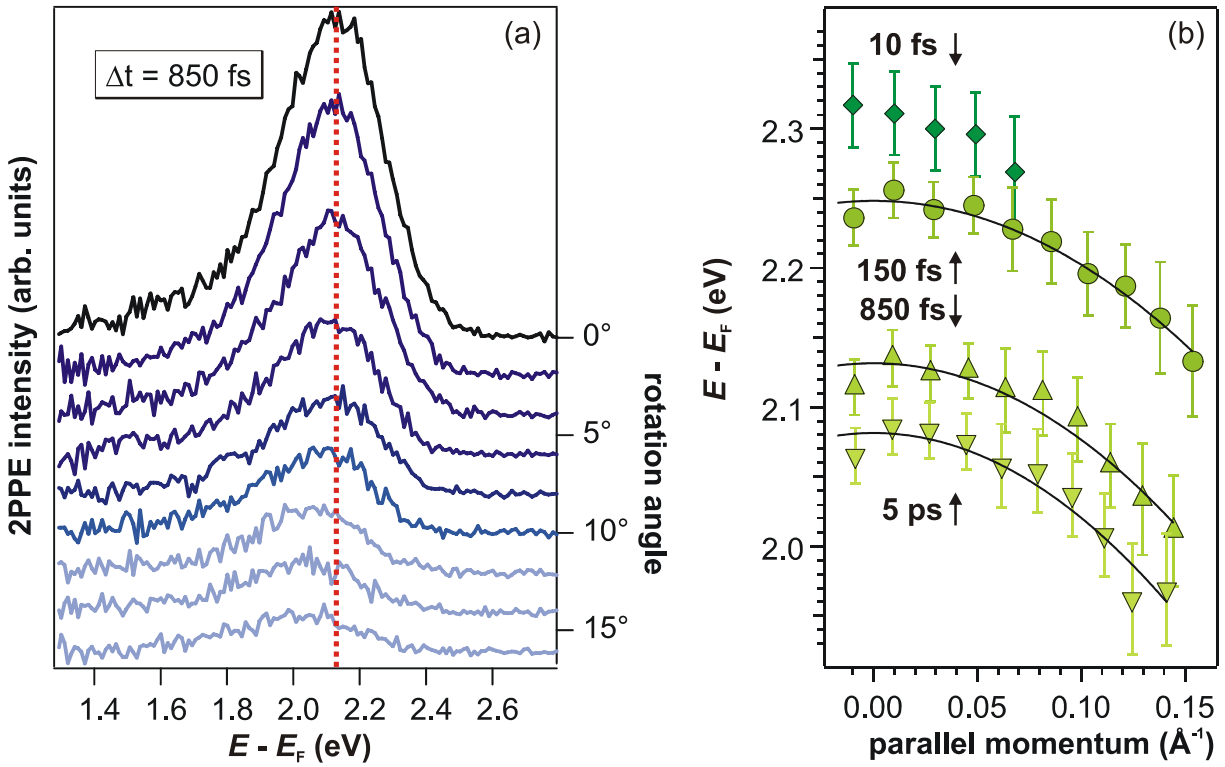

Fig. A.03: *Dispersion of Solvated Electrons in Amorphous Ammonia.* a) Angle-resolved 2PPE spectra at 850 fs time delays. The peak maximum of the solvated electron distribution shifts to lower energies with increasing emission angle. b) The dispersion of e_S is at all time investigated time delays negative. Red and black curves are guides to the eye. See text for details.

However, even at earlier times (t = 10 fs, diamonds in Fig. A.03b) the e_S distribution exhibits a negative dispersion. Due to the strong, time- and angle-dependent background it was not possible to evaluate the peak position at $k_{\parallel} > 0.07$ Å^{-1}. As the observation of an apparent negative dispersion is in agreement with the dispersion measurements of D_2O/Cu(111), it can be concluded that the ammoniated electrons at the NH_3/Cu(111) interface are localized 150 fs after photoinjection. Apparently, the electrons localize considerably directly after photoexcitation.

Appendix B: The First Bilayer of D_2O/Ru(001)

The detailed adsorption structure of the first bilayer of D_2O/Ru(001) is still under discussion as introduced in paragraph 2.4.3. The starting point of the debate was the observation of a smaller vertical distance of the oxygen atoms in the two half layers of the first bilayer by LEED measurements. [Hel94] On the basis of DFT calculations a half-dissociated structure was suggested [Fei02] and SFG experiments indicated an H-down structure without dissociation [Den03]. However, the calculated work functions for the two structures do not coincide with the measured value of 4.15 eV. [Gah04]

Recent theoretical [Men05] and experimental studies [Far05] indicate a convergence of the controversy: It could be shown by *ab initio* DFT calculations that the half-dissociated structure is indeed the energetically most favorable, but, however, the dissociation barrier is with 0.62 eV higher than the adsorption energy of the D_2O. Mixed D-up and D-down arrangements of the bilayer reproduce the measured work function change quite well. [Men05] Faradzhev *et al.* could show that the first D_2O bilayer on the Ru(001) surface is very sensitive to electron irradiation, which leads to subsequent D_2O dissociation. [Far05] They performed thermal desorption (TD) spectroscopy of the D_2O/Ru(001) interface as a function of electron exposure (0-180 eV) and found a significant change of the TD spectra. These experiments have been repeated in the present work. The results are depicted in Fig. B.01 and reproduce the observations of Faradzhev *et al.* very well. The graph shows TD spectra of 1 BL D_2O/Ru(001) without (black) and after irradiation with 180 eV electrons (blue).[116] The desorption peak of the first bilayer lies below 180 K. As introduced in paragraph 3.3.2, the TD spectrum exhibits a high-temperature peak at ~200 K, which is due to oxygen

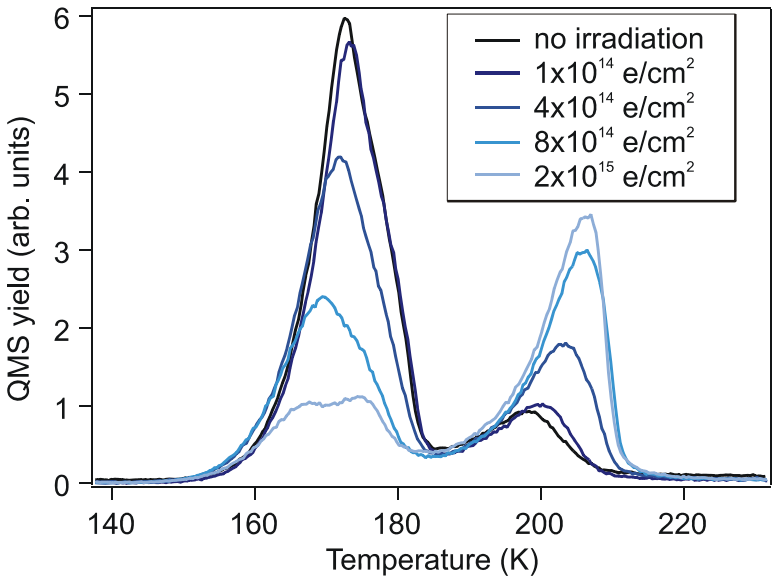

Fig. B.01: *TD Spectra 1 BL D_2O/Ru(001) Before and After Electron Irradiation.* The observed intensity redistribution reproduces the observations in [Far05]. Heating rate: 0.2 K/s. See text for details.

[116] An electron dosage of $1.3 \cdot 10^{15}$ e/cm² corresponds to one electron per D_2O molecule.

contaminations of the D_2O. Irradiation of the sample with electrons[117] leads to an intensity redistribution in favor of the high-temperature peak. For electron densities larger than 10^{15} e/cm^2 the high-temperature feature becomes considerably larger than the "original" bilayer peak. The TD spectra are thus dominated by recombinative desorption of dissociated D_2O/Ru(001). The dissociated D_2O is indeed more strongly bound to the Ru(001) substrate than the molecular ice, as it desorbs at higher sample temperatures.

However, as DFT calculations predict a work function of the half-dissociated structure that ~1 eV higher than the measured value of 4.15 eV, [Fei02, Gah04, Men05] determination of the sample work function as a function of electron exposure is desirable. In addition to the reproduction of the TD spectra of Faradzhev *et al.*, such a work function measurement has been performed in the present work to study possible work function changes upon electron irradiation. The results are depicted in Fig. B.02. Two datasets (circles and diamonds) reveal a linear dependence of the sample work function on the electron exposure.[118] The work function increases with a rate of $3 \cdot 10^{-19}$ eV·electrons/cm^2. After irradiation with $3 \cdot 10^{18}$ electrons/cm^2 the work function reaches the calculated value for the half-dissociated structure of 5 eV. However, it has to be noted, that the electron dosage required for this significant work function change is one thousands times larger than the necessary number of electrons for TD spectra variation. To achieve this drastic change of work function, the sample was irradiated for 16 min with electrons of 180 eV kinetic energy. Recalling that the debate about the bilayer adsorption began due to LEED experiments, an irradiation time of 16 min appears reasonable.

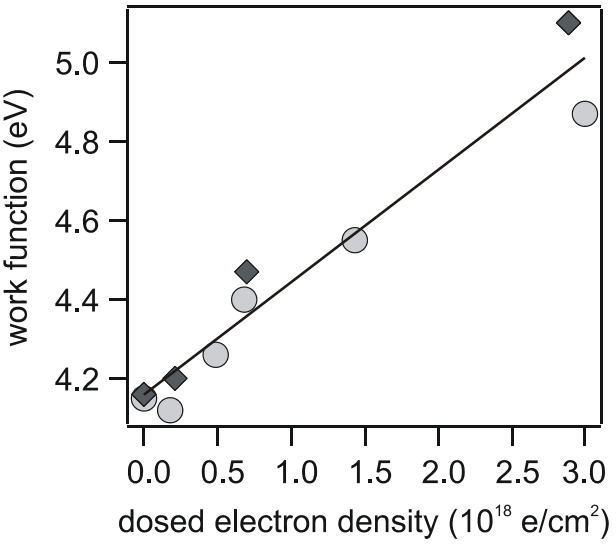

Fig. B.02: *Work Function Change as a Function of Electron Irradiation.* The work function rises linearly with increasing electron exposure. See text for details.

Based on these results, the above scenario for D_2O adsorption of the first bilayer on Ru(001) is supported: The ice adsorbs molecularly on the substrate due to the high dissociation barrier. However, the more stable, half-dissociated structure is achieved by bombardment of the sample with electrons of 180 eV kinetic energy. This structural transition is accompanied by an increase of the sample work function with rising electron exposure. The distance variation of the oxygen atoms observed by Held and Menzel in 1994 probably indeed results from half-dissociated

[117] Irradiation was performed using the LEED spectrometer in the UHV chamber. Electron exposure was determined by measuring the current flow from the sample.

[118] As the electron beam exhibits a varying intensity, the work function differs over the whole sample area. The plotted data is the *mean* value of the sample work function.

D_2O/Ru(001). However, LEED experiments performed in [Hel94] apparently did not image the adsorption structure of D_2O/Ru(001) occurring under electron-free conditions. Therefore, the reduced O-O distance of Held and Menzel's work must not necessarily be taken into account when discussing the non-dissociated structure occurring under contamination-free conditions.

Appendix C: Temperature Calibration

The measurement of low temperatures with thermocouples is challenging, as the thermovoltage varies only slightly with temperature for $T < 100$ K. In the present setup NiCr/Ni thermocouples (type K) were employed, which are officially calibrated down to 4 K. However, depending on the spot welding of the couple and influenced by other junctions, the measured thermovoltage might deviate from the standard calibration. Thermal desorption spectroscopy of rare gases on metal surfaces is a powerful tool to ensure proper temperature measurement, as they adsorb only due to Van der Waals Interaction and therefore desorb at very low temperatures.[119]

Fig. C.01 depicts TD spectra of xenon, krypton, and argon on the Cu(111). The green curves result from the standard calibration. The red arrows indicate literature values for the desorption maxima of the first and second monolayer peaks. [Hot99, Ber04] Obviously, the maxima of the measured TD spectra, calibrated following the standard calibration curve, deviate significantly from these values. Therefore, a recalibration of the thermocouple was performed to ensure reliable temperature measurements.

The literature values for the desorption maxima are plotted versus the measured thermovoltage in Fig. C.02 (markers). The standard calibration curve (dotted line) is a polynomial of eleventh order. [Nis03] The new calibration was achieved accordingly and fitted to the data (black curve). The TD spectra of the rare gases resulting from the new calibration are depicted by the black curves in Fig. C.01. Obviously, the data agrees quite well with the literature values for the desorption maxima.

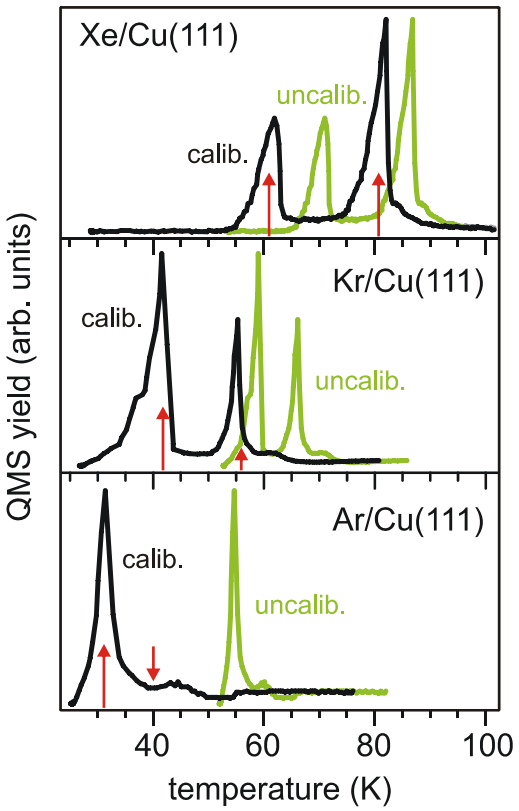

Fig. C.01: *TD Spectra of Rare Gases Adsorbed on Cu(111).* The spectra plotted versus the established temperature calibration (green) deviate significantly from the literature (red arrows). Recalibration of the thermocouple leads to good agreement between results and literature (black curves). See text for details.

[119] The weak interaction with the substrate leads to comparable desorption temperatures for several metals as Cu(111), Ru(001), and Cu(001).

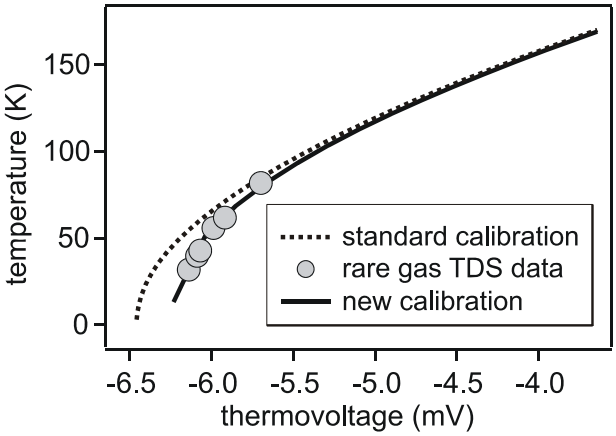

Fig. C.02: *Temperature Calibration.* The standard calibration (dashed curve) deviates from the measured thermovoltages of the rare gas desortion maxima (markers). The new calibration is achieved by fitting a polynomial to the data (black curve).